Energy Reports 8 (2022) 1696–1703

Contents lists available at ScienceDirect

Energy Reports

journal homepage: www.elsevier.com/locate/egyr

Development of cost-effective PCM-carbon foam composites for thermal energy storage

Xin Liu [a], Fangming Yang [a,b], Mengbin Li [a], Chenggong Sun [a], Yupeng Wu [a,*]

[a] Faculty of Engineering, University of Nottingham, Nottingham NG7 2RD, UK
[b] School of Energy and Power Engineering, Shandong University, Jinan, PR China

ARTICLE INFO

Article history:
Received 2 November 2021
Received in revised form 6 December 2021
Accepted 21 December 2021
Available online xxxx

Keywords:
Carbon foam
Thermal energy storage
Phase change materials
PCM composites

ABSTRACT

Phase Change Materials (PCMs) has gained considerable interest for storing thermal energy originating from the solar irradiation, industrial waste heat and surplus heat. Here, we present the facile and scalable synthesis of PCM-carbon foam composites by using polyisocyanurate (PIR) foam derived carbon foam as porous support. The unique 3D molecular configuration of the carbon foam materials embedded the composites with high PCM loading capacity, excellent shape stabilization and thermal reliability and chemical stability. The carbon foams prepared by facile chemical activation method with high surface area up to 1968 m^2/g exhibit high PCM loading capacity of up to 90.8 wt% and excellent energy storage capacity of up to 105.2 J/g. Advanced characterization demonstrated that the total pore volume of carbon foam governs the PCM loading capacity as well as the energy storage performance of the composites. This work provides a potential pathway to recycle PIR foams, which have been widely used in construction industry, by producing cost-effective PCM composites for thermal energy storage.

Contents

1. Introduction 1696
2. Experimental 1697
 2.1. Preparation of PIR-derived carbon foam 1697
 2.2. Preparation of PCM-carbon foam composites 1697
 2.3. Characterizations 1698
3. Results and discussion 1698
 3.1. Preparation of 3D carbon foams using PIR foam 1698
 3.2. Preparation of PCM-carbon foam composites 1699
 3.3. Thermal properties of PCM-carbon foam composites 1701
4. Conclusions 1701
Declaration of competing interest 1702
Acknowledgments 1702
References 1702

1. Introduction

Thermal energy storage based on Phase Change Materials (PCMs) has become an attractive option to meet growing energy demand, with organic PCMs leading the way (Yang et al., 2019). Organic PCMs that can absorb and release thermal energy at a constant temperature during a solid-liquid phase transition exhibit unique advantages such as high energy storage densities, controllable operation temperatures, non-toxicity, no phase separation, a low degree of supercooling, which can be potentially used for storing thermal energy originating from the solar irradiation, industrial waste heat and surplus heat (Sharma et al., 2009; Zhang et al., 2018). However, the inherently low thermal conductivity and potential leakage problem of PCMs at melt stage during phase transition have been the main drawback that limiting their practical applications (Yang et al., 2019; Li et al., 2016b). Microencapsulation of organic PCMs by using polymers such as polystyrene, poly (methyl methacrylate) as shell can minimize the leakage problem of PCMs but is restricted by the low thermal conductivity and high flammability of the polymer shell (Oya

* Corresponding author.
E-mail address: Yupeng.Wu@nottingham.ac.uk (Y. Wu).

https://doi.org/10.1016/j.egyr.2021.12.065

et al., 2012). Dispersed filler with high thermal conductivity including carbon nanotubes, graphite has been used to increase the thermal conductivity of PCMs while large amounts of fillers have to be added, especially in the case of non-carbon fillers, which in turn reduces the energy storage density (Wilson et al., 2019).

To overcome these shortcomings, an alternate approach has been explored by impregnating PCMs in a thermally conducting 3D structural materials (Yang et al., 2017; Li et al., 2016a; Yang et al., 2016; Zhang et al., 2017; Xiao and Zhang, 2013; Ji et al., 2014). The interconnected and thermally conductive 3D skeletons could greatly improve the thermal conductivity and the shape stability of PCMs during the phase transition (Ji et al., 2014). Among different 3D structural materials, carbon-based materials including carbon foams, carbon aerogels, graphene foams have been considered as potential and attractive candidates for the preparation of PCM composites owing to their unique advantages including low thermal expansivity, high thermal and chemical stability, excellent thermal and electrical conductivity (Feng et al., 2016; Balandin, 2011; Novoselov et al., 2012). Numerous precursors including biomass-based materials (Tan et al., 2016; Wei et al., 2018; Fang et al., 2017; Karthik et al., 2015; Li et al., 2014; Zhao et al., 2018), synthetic polymer (Wilson et al., 2019) and graphite/graphene (Ji et al., 2014; Kholmanov et al., 2015; Zhong et al., 2010; Giménez et al., 2017; Tang et al., 2017) have been used to prepare carbon foams. Fang et al. employed a chitosan-derived carbon aerogel prepared via a freeze drying-carbonization process as the supporting material to fabricate form-stable PCMs and both high energy storage capacity and thermal conductivity were achieved (Fang et al., 2017). Karthik et al. reported the fabrication of carbon foam by using synthetic polymer and polyurethane foam as carbon source and sacrificial macroporous template and the prepared erythritol-carbon foam composites has a latent heat of 251 J/g and melting point of 118 °C (Karthik et al., 2015). Li et al. reported the development of carbon aerogel by using watermelon as raw materials via a hydrothermal carbonization-freeze drying-pyrolysis process and paraffin-carbon aerogel composites was successfully prepared with the maximum paraffin loading level of up to 95 wt% and high melting enthalpy of 115.2 J/g (Li et al., 2014). Zhao et al. prepared shape-stable and high-thermal conductivity composite phase change materials by using potatoes and white radishes derived carbon foam as support. The prepared composites exhibited high-thermal conductivity and excellent thermal reliability (Zhao et al., 2018). Ji et al. developed ultrathin-graphite (UGF) foams with large pore volume via chemical vapour deposition method using nickel foam as hard template. The prepared UGF-paraffin wax composites demonstrated high PCM loading level up to 98.2 wt% and the thermal conductivity was increased by up to 18 times (Ji et al., 2014).

The brief literature survey suggests that the carbon-based 3D structural materials have shown great potential in preparation PCM composites for thermal energy storage while most of the current 3D structural carbon-based foams used in preparation of PCM composites normally suffer from high cost or complex synthetic protocol involving multiple complex processes such as ultrathin-graphite foams, carbon aerogels. Therefore, developing cost-effective and nontoxic foam structure is of interest. In the UK, building insulation foams including polyurethane, polyisocyanurate and phenolic foam have been widely used in construction industry due to their light weight, tailor made properties, and corrosion resistance (Feldman, 2010). However, the waste created as off-cuts and as surplus materials at the end of the project have increasingly become a problem in the UK. It is estimated that foam waste will exceed 1 million m^3, or 30 000 tonnes per annum by 2020 (WRAP, 2013). And 4%–7% of the total new production is scrapped and goes to landfill. Estimates suggest that the costs of disposing of the waste foam are of the order of £20 million/annum the producers of foam panels and insulation blocks (Kholmanov et al., 2015). Those insulation foams normally have unique 3D structure with controllable cell size and low density, which can be a potential precursor to produce carbon foam as support to prepare composite PCMs. Here, we present for the first time the facile and scalable synthesis of PCM-carbon foam composites by using insulation materials polyisocyanurate (PIR) foam derived carbon foam as porous support. The unique 3D molecular configuration of the carbon foam materials is expected to endow the composites with high PCM loading capacity and stability and excellent energy storage performance.

2. Experimental

2.1. Preparation of PIR-derived carbon foam

The preparation of PIR-derived carbon foam involved a two-step process. Firstly, polyisocyanurate (PIR) foam bought from local merchant was firstly oxidized according to our previously reported method (Liu et al., 2020). In a typical procedure, a certain amount of PIR foam was placed in a horizontal tube furnace at 260 °C under air flow of 50 ml/min for 6 h. In the second step, two approaches including direct carbonization and chemical activation of oxidized PIR foam were used to obtain the final carbon foam. For direct carbonization, oxidized PIR foam sample was heated up from room temperature to pre-set temperature of 600 and 800 °C in a flow of nitrogen at a heating rate of 5 °C/min. The sample was kept at this temperature for 1 h before it was cooled down to room temperature. In addition, carbon foam was also prepared via chemical activation method by using the oxidized foam as precursor and KOH as activating agent. 1 g of oxidized foam was mixed with 40 ml KOH solution containing 1 g of KOH at ambient temperature for 24 h before it was dried at 110 °C overnight. The dried sample was then placed in a horizontal tube furnace and heated up in a nitrogen flow of 1 L/min to pre-set temperature at a heating rate of 5 °C/min and kept for 1 h. The sample was then collected after it had cooled to ambient temperature and was washed with DI water until a neutral filtrate was obtained. The final product was then dried in an oven at 110 °C overnight. For convenience, the PIR foam prepared by carbonization and activation were labelled as Cx and CxK, respectively, where x represents the carbonization/activation temperature, K means KOH activation.

2.2. Preparation of PCM-carbon foam composites

PCMs with a phase change range compatible with the human thermal comfort temperature (22–28 °C) is particularly suitable for modern built environment applications, which allows the utilization of latent heat to improve the thermal inertia. In this research, PCM, Rubitherm RT28, with a melting/freezing temperature of 26–28 °C was selected. PCM/carbon foam nanocomposite was prepared by using a vacuum impregnation method (Shang et al., 2018; Nomura et al., 2009) and the schematic diagram for preparation of PCM composites using PIR foam is shown in Fig. 1a. 0.5 g of dried carbon foam and 50 g of PCM, Rubitherm RT28, were added into a glass beaker. The mixture was then placed in a pre-heated vacuum oven at 60 °C for 2 h under ambient pressure to ensure that the PCM was completely melt. The sample was kept for another 4 h at 60 °C under vacuum. The impregnated PCM composite was then transferred from the beaker to a piece of filter paper and kept at 60 °C in the vacuum oven. The filter paper was replaced every hour until no liquid PCM leakage was observed. The PCM loading level was calculated as the mass change of carbon foam before and after impregnation.

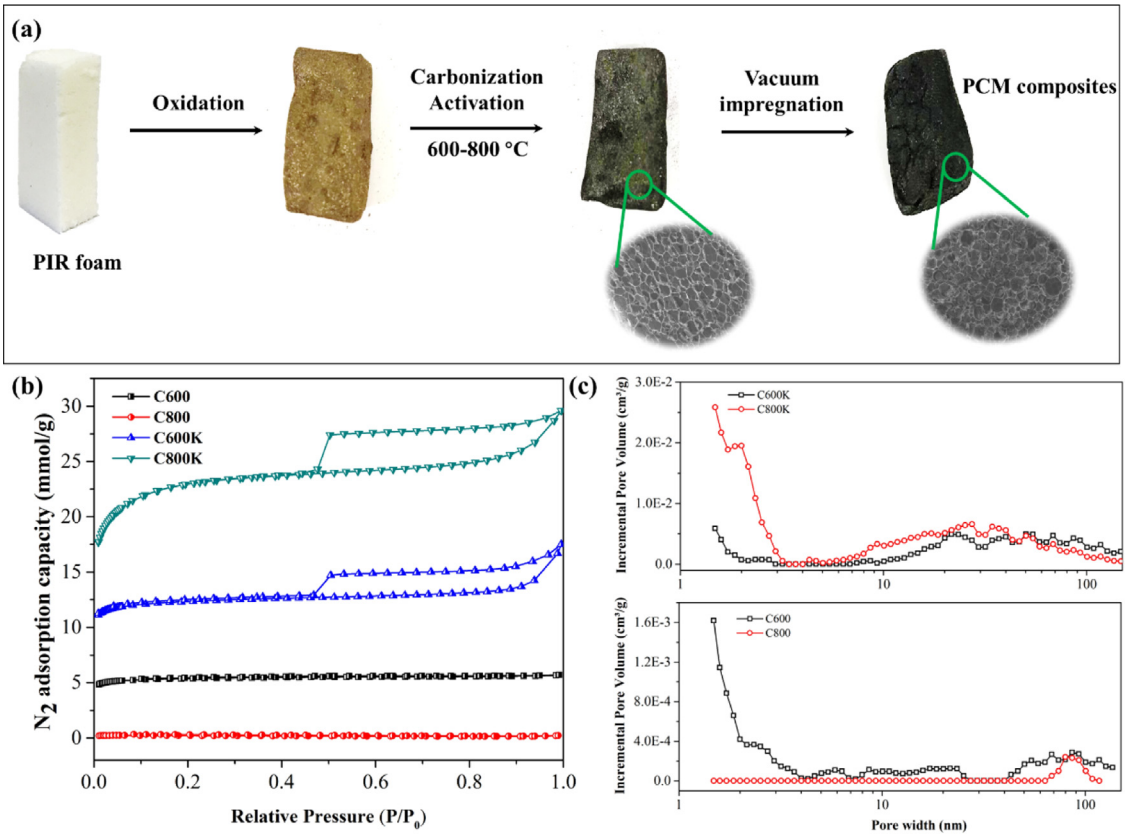

Fig. 1. (a) schematic diagram for PCM composites preparation using PIR foam; (b) N_2 adsorption isotherms of carbon foams; (c) PSDs of carbon foams.

2.3. Characterizations

Micrometrics ASAP 2420 was used to measure the N_2 isotherms of the prepared samples at −196 °C. Before taking the measurements, the samples were first degassed at 120 °C for 16 h. The N_2 adsorption isotherm at P/P_0 of ca. 0.99 was used to calculate the total pore volume. Density functional theory (DFT) model that has been widely used for calculating the pore size distribution of porous materials with a wide range of pore sizes (0.5–100 nm) was selected to analyse the pore size distribution of carbon foam samples from their N_2 adsorption isotherms (Ravikovitch et al., 1998; Do and Do, 2003). The morphology of selected samples was obtained by using JEOL 7000F FEG-SEM. Differential scanning calorimeter (DSC), DSC2500, was used to evaluate the phase change properties of pure PCM and PCM-carbon foam composites. The DSC measurements were conducted in nitrogen atmosphere at a 5 °C/min heating and cooling rate with a temperature ranging from 5 to 60 °C. Thermal stability of carbon foam composites were studied by using TGA (Q500) in the temperature range of 20-600 °C at a heating rate of 5 °C min^{-1} under nitrogen atmosphere.

3. Results and discussion

3.1. Preparation of 3D carbon foams using PIR foam

Fig. 1 shows the nitrogen isotherms of carbon foams prepared under different conditions. It can be found that the direct carbonization of pre-oxidized PIR foam at 600 °C displays type I isotherm with well-defined plateaus at low relative pressure, indicating the purely microporous nature of C600. However, when the carbonization temperature increased to 800 °C, the nitrogen adsorption capacity sharply dropped to about zero, which is presumably due to the widening of micropores formed at low temperature into macropores that could not be measured by gas adsorption method (Leng et al., 2021). In contrast, chemical activation benefits the development of microporosity, the nitrogen adsorption capacity sharply increased over 3 times from about 5 (C600) to 15 mmol/g (C600K) at carbonization temperature of 600 °C. With further increase of activation temperature to 800 °C, the nitrogen adsorption capacity increased to over 27 mmol/g. When chemical activation was employed, the carbon foam samples remain type I isotherm while mesoporosity starts to develop as shown by the emerging of hysteresis loop at high relative pressure. Analysis of the pore size distribution of the carbon foams demonstrates that carbon foams prepared by direction carbonization are predominantly microporous with most of the pores smaller than 2 nm. In comparison, the samples prepared with KOH activation exhibit micro/meso/macroporous hierarchical structure with mesopores/macropores being in the range between 10–100 nm. Both micropore and mesopore volume were significantly improved by chemical activation.

Table 1
Textural properties of carbon foams prepared under different conditions.

Sample	S_{BET} (m^2/g)	V_{total} (cm^3/g)	V_{micro} (cm^3/g)	D_p (nm)
C600	484	0.163	0.155	1.64
C800	22	0.006	0.005	1.34
C600K	1107	0.480	0.350	2.19
C800K	1968	0.820	0.630	2.07

Note: S_{BET}: BET specific surface area; V_{total}: total pore volume; V_{micro}: micropore volume; D_p: average pore diameter.

Table 1 summarizes the textural properties of all carbon foams. The BET surface area and pore volume of carbon foams prepared by direct carbonization sharply dropped from 484 m^2/g and

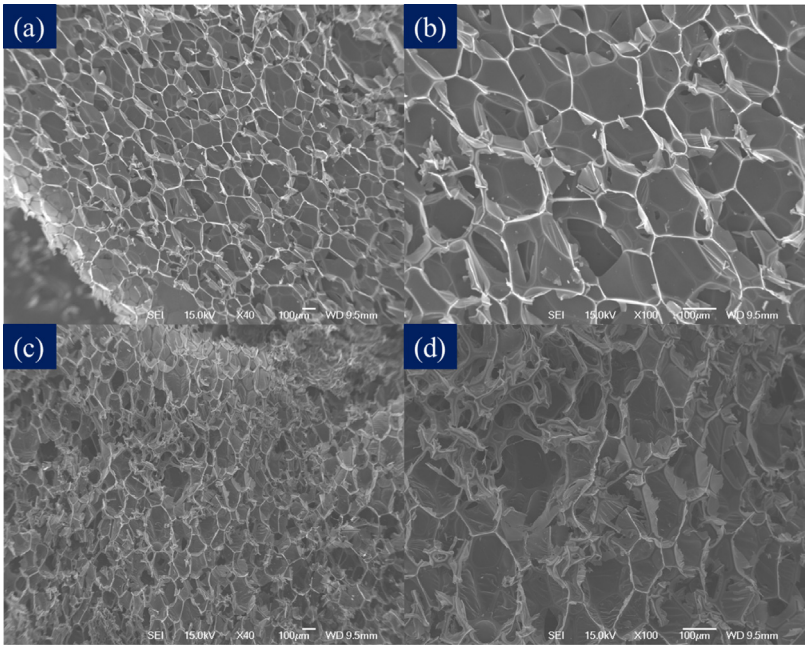

Fig. 2. SEM images of PIR-derived carbon foams prepared by using different approaches with different magnifications: direct carbonization (C600) (a) x40, (b) x100; Chemical activation (C600K) (c) x40, (d) x100.

0.163 cm^3/g to only 22 m^2/g and 0.006 cm^3/g, respectively, as the temperature increases from 600 to 800 °C. However, when chemical activation was employed, the carbon foams exhibited much higher pore volume and surface area than their corresponding counterparts via direct carbonization. For instance, the BET surface area and total pore volume of C800K reached 1968 m^2/g and 0.82 cm^3/g, respectively, which was much higher than C600 and C800. The mesopore and macropore volume of C800K (V_{total} – V_{micro}, 0.19 cm^3/g) was even higher than the total volume of C600. Moreover, chemical activation leads to the widening of pores as the average pore size increased from 1.34–1.64 nm to 2.07–2.19 nm. These results are in consistent with those reported in the literature where KOH activation could enhance the formation of microporosity in carbonaceous materials (Liu et al., 2020; Wang and Kaskel, 2012). The activation process involves a variety of chemical reactions between KOH and carbon to develop porosity of carbon, which could be divided into three groups: (1) carbon fragments are etched by KOH and related potassium compounds (K_2CO_3, and K_2O) formed during activation process; (2) the reactions of carbon with CO_2 and H_2O (steam) produced from KOH decomposition; (3) the formed metallic potassium at temperatures higher than 700 °C could be intercalated into the carbon matrix so as to expand the carbon lattices (Wang et al., 2017; Chen et al., 2020). Being different to direct carbonization, the KOH activation efficacy increases with increasing activation temperature, leading to enhanced porosity of carbonaceous materials (Liu et al., 2019). As shown in Table 1, at the same KOH/PIR foam mass ratio of 1, the surface area and pore volume of carbon foam prepared at 800 °C was much higher than that of carbon foam prepared at much mild temperature of 600 °C. The morphology of the selected carbon foams prepared by direct carbonization and chemical activation is shown in Fig. 2. Carbon foam, C600, prepared from PIR foam has highly interconnected pentagonal and hexagonal ring macrostructures, which appeared to originate from the foam precursor. When chemical activation was employed, the microstructure of the carbon foam became disordered, and the ring structures were widened due to the carbon-consuming activation activities induced by KOH.

3.2. Preparation of PCM-carbon foam composites

To achieve maximum PCM loading level of different carbon foams, vacuum impregnation method was employed. Fig. 3a shows the maximum PCM loading level of different carbon foam samples. It is evident that both carbonization temperature and chemical activation play an important role in determining the maximum loading level of carbon foams. For sample prepare by direct carbonization, the PCM loading level of C600 could reach 78.8 wt%, which was higher than that of C800 with lower total pore volume. When chemical activation was employed, the PCM loading level was significantly improved with C600K reaching about 87.9 wt%, which was about 9 wt% higher than that of C600. When the activation temperature increased to 800 °C, PCM loading level of C800K increased to 90.8 wt%. Fig. 3b shows the relationship between pore volume and PCM loading level. It can be seen that an almost linear relationship was observed between total pore volume and PCM maximum loading level. This indicates that chemical activation benefits the development of hierarchical porous structure shown in Table 1 and Fig. 1 with increasing pore volume and pore size from less than 0.163 cm^3/g and 1.64 nm (C600 and C800) to 0.820 cm^3/g and 2.04 nm (C800K), respectively, which increases the loading capability and pore accessibility of carbon foam and therefore boosts the PCM loading level. The morphology of PCM-carbon foam composites was shown in Fig. 4. It can be found that the PIR carbon foam has suitable porous structure for incorporating liquefied materials and the PCM molecules are successfully loaded into the pores of carbon foam. After PCM impregnation, C600 remains the interconnected pentagonal and hexagonal ring macrostructures. However, the porous structure of C600K seems to be fully occupied by PCM molecules as no clear pentagonal and hexagonal ring macrostructures was observed.

The thermal stability of the composites was evaluated by TGA in the temperature range between 20–600 °C and the results are shown in Fig. 5. Clearly, all composite samples exhibit excellent thermal stability at operating temperature window (<100 °C). The initial small weight loss at temperature lower than 100 °C is attributable to the removal of water from composites. A sharp

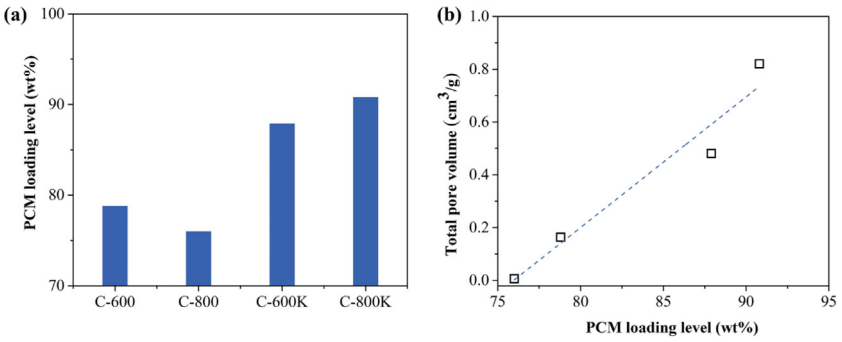

Fig. 3. Preparation of PCM-carbon foam composites: (a) PCM loading level of different carbon foams; (b) the relationship between PCM loading level and total pore volume.

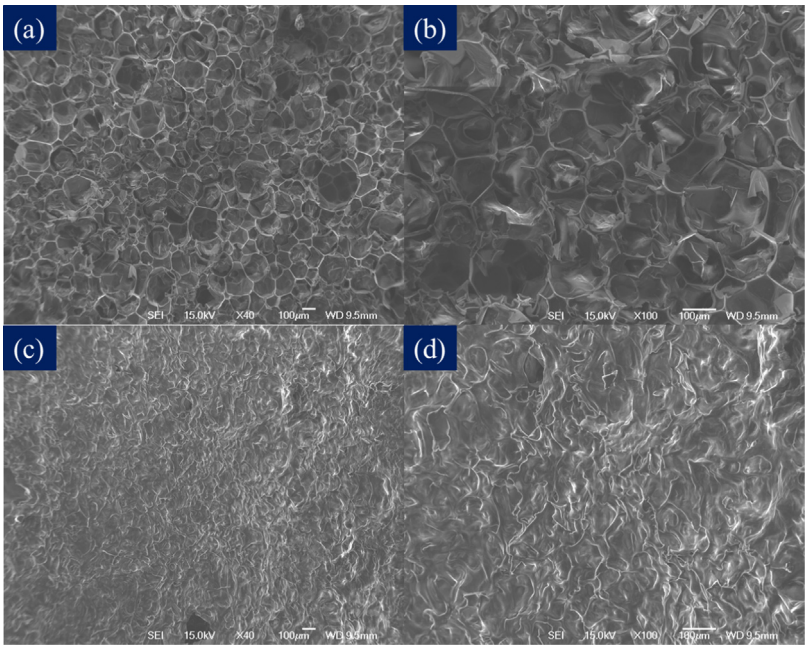

Fig. 4. SEM images of selected PCM-carbon foam composites: (a and b) C600; (c and d) C600K.

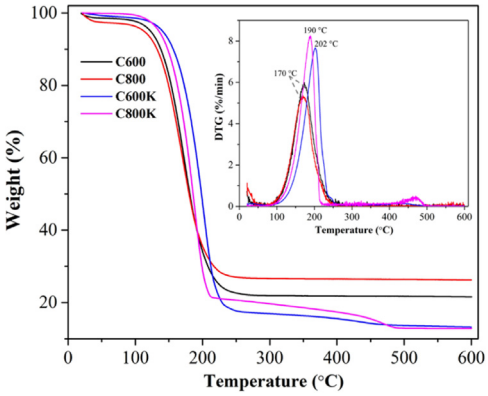

Fig. 5. TGA curves of PCM-carbon foam composites. The inset figure shows the corresponding derivative thermogravimetric (DTG) curves of different composites.

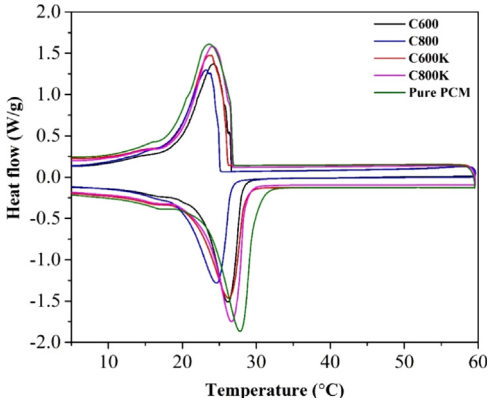

Fig. 6. DSC curves of PCM-carbon foam composites during the heating process and cooling process.

weight loss was observed at the temperature of 120–250 °C, which corresponds to the thermal decomposition of composites. In comparison, the thermal decomposition of PCM-carbon foam composites (C800K and C600K) could be divided into two stages: sharp decrease of weight at temperature between 120–250 °C followed by a slow decomposition process could only achieve less than 10 wt% weight loss between 250–500 °C, the latter being more indicative of the removal of residue PCM molecules

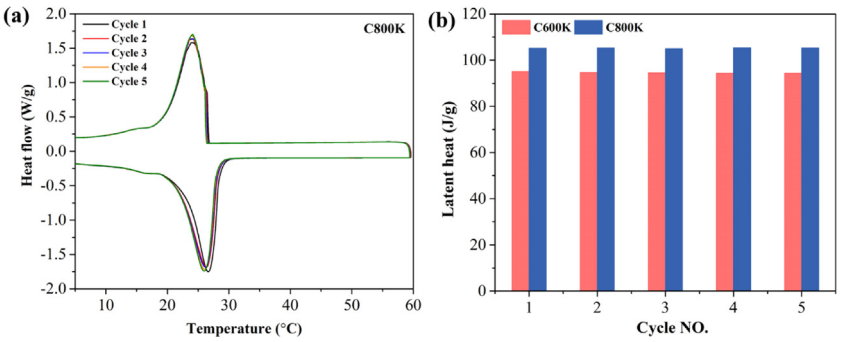

Fig. 7. Cyclic stability test of PCM-carbon foam composites: (a) DSC curves of C800K during melting–freezing cycles; (b) the melting latent heat of C600K and C800K during melting–freezing cycles.

trapped deeply inside the micropores. The DTG curves of different composites show that the peak thermal decomposition temperature of carbon foam composites prepared by using KOH activated carbon foam shifts towards slightly higher temperature from 170 to 190–200 °C, indicating that the PCM molecules trapped inside the micropore is more thermally stable. The peak thermal decomposition temperature of C800K based composites was lower than that of C600K. Given the much higher pore volume and surface area of C800K but only slightly larger PCM loading level (90.8 wt% vs. 87.9 wt%) than that of C600K, much more pore channels inside C800K are accessible that could potentially reduce the diffusion resistance of decomposed compounds from the carbon foam framework to outside and therefore a lower temperature is required for thermal decomposition.

3.3. Thermal properties of PCM-carbon foam composites

Fig. 6 shows the DSC heating and cooling curves of pure PCM and PCM-carbon foam composites, and the thermal characteristics of different carbon foam samples were shown in Table 2. It can be seen that one endothermic peak centred at about 26 °C during the melting of PCM and one exothermic peak centred at 24 °C in the crystallization process was observed for all samples, which corresponds to the melting point (T_m) and freezing point (T_f), respectively. It can be found from Table 2 that the melting and freezing temperature of pure PCM were 27.8 and 23.7 °C, respectively, with a supercooling degree (T_m-T_f) of about 4.1 °C. In comparison, PCM-carbon composites exhibit lower melting temperature but slightly higher freezing temperature, leading to a supercooling degree of only 1.9–2.5 °C. The sharp decrease in supercooling degree of PCM could be attributable to the improvement of thermal conductivity by carbon foam (Wu et al., 2021). As for PCM-carbon foam composites, the melting temperature and the supercooling degree increased from about 24.9 to 26.6 °C and 1.8 to 2.5 °C with the increase of PCM loading level from 76.0 wt% (C800) to 90.8 wt% (C800K). The shift in melting temperature and increase in supercooling degree are presumably due to the physical interaction between PCM molecules and foam structure (Wu et al., 2021). It seems that the microporous dominant structure has stronger interaction with PCM molecules as T_m of C800 with smallest pore volume and surface area was much lower ($\Delta T >$ 1 °C) than other samples. The prepared carbon foam composites have a phase transition temperature of 25-27 °C, which is very close to the human comfort temperature, so it has the potential in building applications.

The melting and freezing latent heat of all carbon foam composites were shown in Table 2. It is evident that the latent heat of PCM-carbon foam composites was affected by the PCM loading level. For instance, the melting latent heat (ΔH_m) increased from 80.5 to 105.2 J/g with the increase of PCM loading level from 76.0 to 90.8 wt%. This indicates that pore volume of carbon foam plays an important role in determining the energy storage capacity of the composites as the PCM loading level increased linearly with the increase of the total pore volume of carbon foam (see Fig. 3b). Chemical activation benefits the development of porosity of carbon foam, which improves the PCM loading level and therefore the energy storage capacity. At a given carbonization temperature of 800 °C, the melting latent heat of composite prepared using C800K was about 105.2 J/g, which is 31% higher than that of composite prepared using C800. Similar trend was observed for freezing latent heat of PCM-carbon foam composites. Among all carbon foam composites, C800K achieves the highest melting and freezing latent heats of 105.2 and 105.4 J/g, respectively, which is among the best PCM composites with similar or slightly higher operating temperature window reported by previous studies (Table 3). In addition to the high energy storage capacity, those composites also demonstrated excellent thermal reliability and chemical stability. As shown in Fig. 7a, the energy storage was fully reversible and no obvious change in thermal properties and chemical structure was observed after 5 melting–freezing cycles. The melting and freezing latent heat of selected composites shown in Fig. 7b remains stable during 5 continuous melting–freezing cycles.

Table 2
Heat energy storage properties of the carbon foam composites.

Sample	T_m (°C)	T_f (°C)	ΔH_m (J/g)	ΔH_f (J/g)	$T_m - T_f$ (°C)
Pure PCM	27.8	23.7	120.2	125.1	4.1
C600	26.1	24.2	85.6	91.0	1.9
C800	24.9	23.1	80.5	84.9	1.8
C600K	26.2	24.0	95.0	91.8	2.2
C800K	26.6	24.1	105.2	105.4	2.5

4. Conclusions

In conclusion, a series of novel PCM-carbon foam composites were designed and developed by using PIR insulation foam derived carbon foam as support and RT28 via vacuum impregnation method. The textural properties of carbon foams are tailorable by tuning the carbonization temperature and chemical activation. The carbon foams prepared by using chemical activation exhibited much higher pore volume and surface area compared to carbon foams obtained via direction carbonization, which is particular favourable for preparation of PCM-carbon foam composites with the PCM loading level reaching up to 91 wt%. The results demonstrated that the PCM-carbon foam composites possess high thermal energy storage capacity of up to 105.2 J/g, which is amongst the highest reported so far. In addition, the composites also had excellent thermal reliability and chemical stability during melting–freezing cycles.

Table 3
Comparison of thermal properties of PCM composites with similar melting/freezing temperature in literatures.

PCM composites	T_m (°C)	T_f (°C)	Latent heat (J/g)	Ref
C600K	26.2	24.0	95.0	This work
C800K	26.6	24.1	105.2	
PEG/diatomite	27.7	32.2	87.09	Karaman et al. (2011)
Paraffin/expanded vermiculite	27.0	25.1	77.6	Xu et al. (2015)
Stearic acid/graphene oxide	32/57	23/49	56.1/43.0	Li et al. (2013)
Capric acid-myristic acid/perlite	21.70	20.70	85.40	Karaipekli and Sarı (2008)
Lauric acid/kaolin	43.7	39.3	72.5	Song et al. (2014)
n-nonadecane/cement	31.9	31.8	69.1	Li et al. (2010)
Octadecane/vermiculite	26.1	24.9	142.0	Chung et al. (2015)
Capric acid/rGO-diatomite	30.5	29.2	106.2	Li and Mu (2019)
Capric-Stearic acid/perlite	30.7	17.2	118.6	Wei et al. (2014)

Declaration of competing interest

The authors declare that they have no known competing financial interests or personal relationships that could have appeared to influence the work reported in this paper.

Acknowledgments

This work was supported by the Engineering and Physical Sciences Research Council, UK [grant number EP/S030786/1, EP/R001308/1] and the UK Carbon Capture and Storage Research Centre (EP/K000446/1). We thank Mr. Kieron Orange for his kind assistance with DSC measurements.

References

Balandin, A.A., 2011. Thermal properties of graphene and nanostructured carbon materials. Nat. Mater. 10 (8), 569–581.
Chen, W., Gong, M., Li, K., Xia, M., Chen, Z., Xiao, H., Fang, Y., Chen, Y., Yang, H., Chen, H., 2020. Insight into KOH activation mechanism during biomass pyrolysis: Chemical reactions between O-containing groups and KOH. Appl. Energy 278, 115730.
Chung, O., Jeong, S.G., Kim, S., 2015. Preparation of energy efficient paraffinic PCMs/expanded vermiculite and perlite composites for energy saving in buildings. Sol. Energy Mater. Sol. Cells 137, 107–112.
Do, D.D., Do, H.D., 2003. Pore characterization of carbonaceous materials by DFT and GCMC simulations: a review. Adsorp. Sci. Technol. 21 (5), 389–423.
Fang, X., Hao, P., Song, B., Tuan, C.C., Wong, C.P., Yu, Z.T., 2017. Form-stable phase change material embedded with chitosan-derived carbon aerogel. Mater. Lett. 195, 79–81.
Feldman, D., 2010. Polymeric foam materials for insulation in buildings. In: Materials for Energy Efficiency and Thermal Comfort in Buildings. Woodhead Publishing, pp. 257–273.
Feng, W., Qin, M., Feng, Y., 2016. Toward highly thermally conductive all-carbon composites: structure control. Carbon 109, 575–597.
Giménez, P., Jové, A., Prieto, C., Fereres, S., 2017. Effect of an increased thermal contact resistance in a salt PCM-graphite foam composite TES system. Renew. Energy 106, 321–334.
Ji, H., Sellan, D.P., Pettes, M.T., Kong, X., Ji, J., Shi, L., Ruoff, R.S., 2014. Enhanced thermal conductivity of phase change materials with ultrathin-graphite foams for thermal energy storage. Energy Environ. Sci. 7 (3), 1185–1192.
Karaipekli, A., Sarı, A., 2008. Capric–myristic acid/expanded perlite composite as form-stable phase change material for latent heat thermal energy storage. Renew. Energy 33 (12), 2599–2605.
Karaman, S., Karaipekli, A., Sarı, A., Bicer, A., 2011. Polyethylene glycol (PEG)/diatomite composite as a novel form-stable phase change material for thermal energy storage. Sol. Energy Mater. Sol. Cells 95 (7), 1647–1653.
Karthik, M., Faik, A., Blanco-Rodríguez, P., Rodríguez-Aseguinolaza, J., D'Aguanno, B., 2015. Preparation of erythritol-graphite foam phase change composite with enhanced thermal conductivity for thermal energy storage applications. Carbon 94, 266–276.
Kholmanov, I., Kim, J., Ou, E., Ruoff, R.S., Shi, L., 2015. Continuous carbon nanotube-ultrathin graphite hybrid foams for increased thermal conductivity and suppressed subcooling in composite phase change materials. ACS Nano 9 (12), 11699–11707.
Leng, L., Xiong, Q., Yang, L., Li, H., Zhou, Y., Zhang, W., Jiang, S., Li, H., Huang, H., 2021. An overview on engineering the surface area and porosity of biochar. Sci. Total Environ. 763, 144204.
Li, Y., Li, J., Deng, Y., Guan, W., Wang, X., Qian, T., 2016a. Preparation of paraffin/porous TiO_2 foams with enhanced thermal conductivity as PCM, by covering the TiO_2 surface with a carbon layer. Appl. Energy 171, 37–45.
Li, H., Liu, X., Fang, G., 2010. Preparation and characteristics of n-nonadecane/cement composites as thermal energy storage materials in buildings. Energy Build. 42 (10), 1661–1665.
Li, B., Liu, T., Hu, L., Wang, Y., Nie, S., 2013. Facile preparation and adjustable thermal property of stearic acid–graphene oxide composite as shape-stabilized phase change material. Chem. Eng. J. 215, 819–826.
Li, M., Mu, B., 2019. Fabrication and characterization of capric acid/reduced graphene oxide decorated diatomite composite phase change materials for solar energy storage. R. Soc. Open Sci. 6 (1), 181664.
Li, Y., Samad, Y.A., Polychronopoulou, K., Alhassan, S.M., Liao, K., 2014. From biomass to high performance solar-thermal and electric-thermal energy conversion and storage materials. J. Mater. Chem. A 2 (21), 7759–7765.
Li, G., Zhang, X., Wang, J., Fang, J., 2016b. From anisotropic graphene aerogels to electron-and photo-driven phase change composites. J. Mater. Chem. A 4 (43), 17042–17049.
Liu, X., Sun, C., Liu, H., Tan, W.H., Wang, W., Snape, C., 2019. Developing hierarchically ultra-micro/mesoporous biocarbons for highly selective carbon dioxide adsorption. Chem. Eng. J. 361, 199–208.
Liu, X., Wang, S., Sun, C., Liu, H., Stevens, L., Dwomoh, P.K., Snape, C., 2020. Synthesis of functionalized 3D microporous carbon foams for selective CO_2 capture. Chem. Eng. J. 402, 125459.
Nomura, T., Okinaka, N., Akiyama, T., 2009. Impregnation of porous material with phase change material for thermal energy storage. Mater. Chem. Phys. 115 (2–3), 846–850.
Novoselov, K.S., Fal, V.I., Colombo, L., Gellert, P.R., Schwab, M.G., Kim, K., 2012. A roadmap for graphene. Nature 490 (7419), 192–200.
Oya, T., Nomura, T., Okinaka, N., Akiyama, T., 2012. Phase change composite based on porous nickel and erythritol. Appl. Therm. Eng. 40, 373–377.
Ravikovitch, P.I., Haller, G.L., Neimark, A.V., 1998. Density functional theory model for calculating pore size distributions: pore structure of nanoporous catalysts. Adv. Colloid Interface Sci. 76, 203–226.
Shang, B., Hu, J., Hu, R., Cheng, J., Luo, X., 2018. Modularized thermal storage unit of metal foam/paraffin composite. Int. J. Heat Mass Transfer 125, 596–603.
Sharma, A., Tyagi, V.V., Chen, C.R., Buddhi, D., 2009. Review on thermal energy storage with phase change materials and applications. Renew. Sustain. Energy Rev. 13 (2), 318–345.
Song, S., Dong, L., Zhang, Y., Chen, S., Li, Q., Guo, Y., Deng, S., Si, S., Xiong, C., 2014. Lauric acid/intercalated kaolinite as form-stable phase change material for thermal energy storage. Energy 76, 385–389.
Tan, B., Huang, Z., Yin, Z., Min, X., Liu, Y.G., Wu, X., Fang, M., 2016. Preparation and thermal properties of shape-stabilized composite phase change materials based on polyethylene glycol and porous carbon prepared from potato. RSC Adv. 6 (19), 15821–15830.
Tang, L.S., Yang, J., Bao, R.Y., Liu, Z.Y., Xie, B.H., Yang, M.B., Yang, W., 2017. Polyethylene glycol/graphene oxide aerogel shape-stabilized phase change materials for photo-to-thermal energy conversion and storage via tuning the oxidation degree of graphene oxide. Energy Convers. Manage. 146, 253–264.
Wang, J., Kaskel, S., 2012. KOH activation of carbon-based materials for energy storage. J. Mater. Chem. 22 (45), 23710–23725.
Wang, J., Nie, P., Ding, B., Dong, S., Hao, X., Dou, H., Zhang, X., 2017. Biomass derived carbon for energy storage devices. J. Mater. Chem. A 5 (6), 2411–2428.
Wei, Y., Li, J., Sun, F., Wu, J., Zhao, L., 2018. Leakage-proof phase change composites supported by biomass carbon aerogels from succulents. Green Chem. 20 (8), 1858–1865.
Wei, T., Zheng, B., Liu, J., Gao, Y., Guo, W., 2014. Structures and thermal properties of fatty acid/expanded perlite composites as form-stable phase change materials. Energy Build. 68, 587–592.
Wilson, P., Vijayan, S., Prabhakaran, K., 2019. Thermally conducting microcellular carbon foams as a superior host for wax-based phase change materials. Adv. Eng. Mater. 21 (4), 1801139.
WRAP, 2013. Building insulation foam resource efficiency partnership: A resource efficiency action plan. http://www.wrap.org.uk/sites/files/wrap/BIF%20REAP%20v2.pdf.

Wu, R., Gao, W., Zhou, Y., Wang, Z., Lin, Q., 2021. A novel three-dimensional network-based stearic acid/graphitized carbon foam composite as high-performance shape-stabilized phase change material for thermal energy storage. Composites B 225, 109318.

Xiao, X., Zhang, P., 2013. Morphologies and thermal characterization of paraffin/carbon foam composite phase change material. Sol. Energy Mater. Sol. Cells 117, 451–461.

Xu, B., Ma, H., Lu, Z., Li, Z., 2015. Paraffin/expanded vermiculite composite phase change material as aggregate for developing lightweight thermal energy storage cement-based composites. Appl. Energy 160, 358–367.

Yang, J., Tang, L.S., Bai, L., Bao, R.Y., Liu, Z.Y., Xie, B.H., Yang, M.B., Yang, W., 2019. High-performance composite phase change materials for energy conversion based on macroscopically three-dimensional structural materials. Mater. Horiz. 6 (2), 250–273.

Yang, J., Yu, P., Tang, L.S., Bao, R.Y., Liu, Z.Y., Yang, M.B., Yang, W., 2017. Hierarchically interconnected porous scaffolds for phase change materials with improved thermal conductivity and efficient solar-to-electric energy conversion. Nanoscale 9 (45), 17704–17709.

Yang, J., Zhang, E., Li, X., Zhang, Y., Qu, J., Yu, Z.Z., 2016. Cellulose/graphene aerogel supported phase change composites with high thermal conductivity and good shape stability for thermal energy storage. Carbon 98, 50–57.

Zhang, P., Meng, Z.N., Zhu, H., Wang, Y.L., Peng, S.P., 2017. Melting heat transfer characteristics of a composite phase change material fabricated by paraffin and metal foam. Appl. Energy 185, 1971–1983.

Zhang, N., Yuan, Y., Cao, X., Du, Y., Zhang, Z., Gui, Y., 2018. Latent heat thermal energy storage systems with solid-liquid phase change materials: a review. Adv. Eng. Mater. 20 (6), 1700753.

Zhao, Y., Min, X., Huang, Z., Liu, Y.G., Wu, X., Fang, M., 2018. Honeycomb-like structured biological porous carbon encapsulating PEG: A shape-stable phase change material with enhanced thermal conductivity for thermal energy storage. Energy Build. 158, 1049–1062.

Zhong, Y., Guo, Q., Li, S., Shi, J., Liu, L., 2010. Heat transfer enhancement of paraffin wax using graphite foam for thermal energy storage. Sol. Energy Mater. Sol. Cells 94 (6), 1011–1014.